EAST EUROPEAN JOURNAL OF PHYSICS. 1. 197-204 (2023)
DOI:10.26565/2312-4334-2023-1-26 ISSN 2312-4334

COMPUTATIONAL INVESTIGATION OF IR AND UV-VIS SPECTRA OF 2-ISOPROPYL-5-METHYL-1,4-BENZOQUINONE USING DFT AND HF METHODS†

Salah M.A. Ridha[a]*, Zahraa Talib Ghaleb[b], Abdulhadi Mirdan Ghaleb[a]
[a]*Department of Physics, College of Science, University of Kirkuk, Kirkuk, Iraq*
[b]*Department of Chemistry, College of Science, University of Kirkuk, Kirkuk, Iraq*
**Corresponding Author e-mail: salahyagmuroglu@uokirkuk.edu.iq*
Received December 16, 2022; revised December 28, 2022; accepted January 5, 2023

A theoretical study on the thymoquinone compound has been performed through two theoretical methods, DFT/B3LYP and HF with 6-31G, 6-31G(d,p) and 6-31++G(d,p) basis sets using Gaussian 09 program. Some theoretical properties, like vibrational and electronic properties especially UV-Vis and FT-IR spectra, of the title compound were analyzed and then compared with available experimental data. The calculated harmonic vibrational frequencies have been scaled with standard scaling factors 0.9 and 0.965 for HF and DFT/B3LYP, respectively and then compared with available experimental FT-IR spectrum. Furthermore, the statistical analysis was investigated to evaluate the performance of both the HF and DFT methods, including root mean square error (RMSE), mean absolute error (MAE) and mean percentage error (MPE). According to the assigned vibrational modes of the title compound, it could be concluded that the DFT/B3LYP method with 6-31++G(d,p) basis set had the best agreement with experimental data. UV-Vis absorption spectra, excitation energies, maximum absorption wavelength, electronic transitions and oscillator strengths of the title compound were calculated by time dependent density functional theory (TD-DFT) method using the same basis set and compared with available experimental data. The results showed the best performer was HF method with 6-31G basis set.
Keywords: *Thymoquinone; DFT; HF; UV-Vis; FT-IR; TD-DFT*
PACS: 87.10.-e, 31.15.A-, 31.15.aj, 31.15.E-, 31.15.ee, 31.15.eg

Nigella sativa L. (Ranunculaceae), better known as black seed or black cumin, is cultivated in many countries of the world in East Africa, the Middle East, Mediterranean countries, South Asia, etc. [1]. 2-isopropyl-5-methyl-1,4-benzoquinone called as thymoquinone is an organic compound with the formula $C_{10}H_{12}O_2$ and its geometric structure with the labeling of atoms are given in Figure 1.

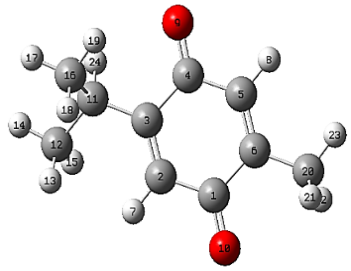

Figure 1. Molecular structure of Thymoquinone compound along with numbering of atoms

It is a derivative of benzoquinone by placement of an isopropyl and methyl groups on carbon 2 and carbon 5, respectively. Thymoquinone (TQ) is an important component of Nigella sativa seed and commercial seed oils, TQ is the main active constituent of black seed oil [2]. Thymoquinone, the main component of black cumin seeds, has been identified from ethanol extract [3]. As first suggested and extracted by El-Dakhakhny in 1965 [4]. Black cumin seeds along with the active ingredient thymoquinone are mainly used for medicinal purposes [5]. With this together, this medicinal plant is effective against cancer of the kidneys, lungs, prostate and liver in the blood system [6]. Also, Nigella sativa gives powerful benefits to many inflammatory cancers such as the liver [7]. N. Sativa oil is considered one of the beneficial oils for human health, thanks to the antioxidant, anti-inflammatory, anti-bacterial activities of these oils, and its active effect on the immune system [8-12].Nigella sativa (black cumin) seeds are also used in traditional medicine to treat a wide range of diseases including diarrhea and asthma [13].Various other studies revealed that the pharmacological activity of Nigella sativa is mainly due to its oil constituent, that are rich in thymoquinone and about 30–48 % of the total content[14].

The main goal of this work was to validate the chemical model that best describes the electronic and spectroscopic properties of TQ molecule. Hence, both Density Functional Theory (DFT) and Hartree-Fock (HF) methods with several basis sets were selected to calculate the electronic and spectroscopic properties, which were compared with experimental results. Furthermore, we checked the relative performance of DFT/B3LYP and HF methods for comparison, at the different 6-31G, 6-31G(d,p), and 6-31++(d,p) levels through statistical study for thymoquinone molecule.

COMPUTATIONAL DETAILS

In this work, all the calculations for Thymoquinone (TQ) molecule were carried at Hartree-Fock (HF) [15] and Density Functional Theory (DFT) using Becke's three-parameter hybrid method [16] with the Lee, Yang, and Parr correlation functional [17] (B3LYP) level with the several basis sets (6-31G, 6-31G(d, p), 6-31++G(d, p)) using the Gaussian 09 W package [18] program for simulation of FTIR and UV-Vis spectra of the title molecule. Gauss-View 5.0 [19] molecular visualization program, a graphical interface was used to assign the vibrational modes for motions observed against fundamental frequencies. The geometrical optimizations, followed by a frequency calculation

† ***Cite as:*** S.M.A. Ridha, Z.T. Ghaleb, and A.M. Ghaleb, East Eur. J. Phys. **1**, 197 (2023), https://doi.org/10.26565/2312-4334-2023-1-26

for the Thymoquinone molecule has been done, using the same basis sets at different level theories and no imaginary wavenumbers were obtained, so the structure is at the minimum energy state. In order to improve the computed values to be in agreement with the observed experimental values, it was necessary to scale down the calculated harmonic frequencies. Hence, the vibrational frequencies calculated at HF and DFT/B3LYP methods were scaled by 0.90 and 0.965 [20], respectively. The theoretical vibrational wave numbers were also plotted with the results obtained by different levels frequency calculations and compared with the experimental IR spectrum.

Simulated Ultraviolet- Visible (UV-Vis) absorption spectra, electronic transition, vertical excitation energies and oscillator strengths for the optimized (TQ) molecule were computed at different levels in each method by the Time Dependent - Density Functional Theory (TD-DFT) using the same basis sets, then compared with the experimental UV-Vis spectrum.

RESULTS AND DISCUSSION

Vibrational Frequencies

Vibration frequencies calculated by HF and DFT/B3LYP with the several basis sets (6-31G, 6-311G(d,p), 6-31++G(d, p)) for the title compound are listed in Table 1. The calculated spectra by DFT/B3LYP method are in a better agreement than HF method with the experimental one. A general better performance of DFT/B3LYP versus HF at 6-31++G(d, p) basis set can be quantitatively characterized by using the calculated mean percentage error (MPE), mean absolute error (MAE), and root mean square error (RMSE) between the calculated and observed vibrational frequencies are presented in Table2, also histograms of the errors are shown in Figures 2 and 3. It is not surprising that the HF frequencies are in poor agreement with the experimental vibrational modes compared to the other theoretical DFT/B3LYP method. This expectation is due to the neglect of electron correlation in HF calculations. After scaling, the HF calculations are in much better agreement, showing a noticeable decrease in the RMSE, MAE and MPE of around 146-151 cm^{-1}, 137-145 cm^{-1} and 9-11 cm^{-1}, respectively. Also, as shown in Table2, the effect scaling factor on the errors in the HF frequencies where the agreement for un-scaled frequencies is strongly skewed toward overestimation. In contrast to HF method, the errors for DFT/B3LYP are shown in Table 2, show that the calculated vibrational frequencies are closer to the experimental ones than the HF method at all basis sets used in this study. As we noted the DFT/B3LYP method at 6-31++ G(d, p) basis set is the most successful procedure for predicting vibrational frequencies in agreement with experimental fundamentals. All methods show an improved errors from scaled IR data. The effect of scaling factor and basis sets on the errors is evident from Figures 2-3, where the histograms for DFT/B3LYP and HF methods show a noticeable improvement using scaling factor and high levels of basis sets.

The (IR) infrared spectrum of the title compound (TQ) has been previously reported [21]. The spectra obtained from scaled HF and DFT/B3LYP methods at different basis sets are shown in Figure 4. After we were applied the scale factor for HF and DFT/B3LYP methods, we observed a good agreement between the experimental and the calculated values. These results indicate that the DFT/B3LYP calculation at 6-31++G(d, p) basis set approximate the observed vibrational modes much better than the HF results. Therefore, the theoretical calculations will be discussed with the experimental results based on the DFT/B3LYP method at the basis set 6-31++ G(d,p). The small deviation between experimental and calculated vibrational modes can be come from the theoretical calculations belong to gaseous phase and experimental results belong to solid phase.

The characteristic strong band due to carbonyl group stretching of a cyclohexadiene was observed near 1655$cm^{-1}$and the respective calculated band is assigned at 1659 cm^{-1}, which is supported by previous studies with values of (1648 cm^{-1}) and (1661cm^{-1}) for thymoquinone and 1,4 benzoquinone, respectively [21,22]. In the methyl groups, three observed bands occur at 2878, 2928, and 2970 cm^{-1}**;** bands 2878 and 2928 cm^{-1} attributed to symmetric stretching and the band at 2970 cm^{-1} arises from asymmetric stretching, and the value previously reported [21] was 2969 cm^{-1} while computations predicts these modes at 2930, 2933, and 3001 cm^{-1}. Also, two types of bending vibrations can be observed in the methyl groups, one of them is a symmetric bending vibration that includes in phase bending and the other anti-symmetric bending vibration which includes out-of-phase bending of C-H bonds. The symmetrical bending vibration (δ_sCH3) occurs near 1360 cm^{-1} (calculated 1360 cm^{-1}), the anti-symmetrical bending vibrations (δ_{as}CH3) near 1437 cm^{-1}(calculated 1431 cm^{-1}) and 1461 cm^{-1}(calculate 1463 cm^{-1}) and the values previously reported [23] were 1375 cm^{-1} and 1450 cm^{-1} for the anti-symmetrical and symmetrical bending vibrations, respectively.

The weak band observed at wavenumber 3050 cm^{-1} was attributed to C-H stretching vibration in the vinyl C-H (C=C-H groups) and respective calculated band at 3080 cm^{-1} which had previously been reported [22] at 3058 cm^{-1}.The out-of-plane bending bands of the vinyl(two C-H groups) are observed at 808 cm^{-1} and 871 cm^{-1} (calculated 846 and 907 cm^{-1}), 783 and 832 cm^{-1} for γ-Trepinene [24]. These two bands are partially mixed with the rocking motion of the methyl groups linked to the ring. In the spectral range region (1300-1000 cm^{-1}), the bands observed at 1024 cm^{-1} which is due to the stretching $C3_{ring}$ – $C(CH3)_2$ bond (calculated 999 cm^{-1}), 1104 cm^{-1}, 1180 cm^{-1} and 1247 cm^{-1} (in plane bending of the vinyl C-H (C = C-H groups); calculated 1110, 1197 and 1218 cm^{-1}, respectively) and 1304 cm^{-1} for the $(C\text{-}C)_{ring}$ stretching band (calculated 1325 cm^{-1}). The recognition of C=C stretching band is an exceptionally troublesome task, since the strong C=O stretching band in title compound is present in this frequency range. The C=C stretching band in 1,4-cyclohexadiene has been observed at wavenumber 1640 cm^{-1}which contains no methyl and isopropyl substituents, while in γ-Trepinene [24] at 1670 cm^{-1} which contains no oxygen atoms substituent; however, the medium band observed at 1615 cm^{-1} belong to C=C stretching band while the calculated value appeared at 1604 cm^{-1}.

Table 1. Experimental and calculated IR spectral data of the title compound together with their assignments

No.	Observed frequency*	Calculated frequency (cm-1)with DFT/B3LYP/ 6-31G			Calculated frequency (cm-1)with DFT/B3LYP/ 6-31G (d,p)			Calculated frequency (cm-1)with DFT/B3LYP/ 6-31+ + g(d, p)			Calculated frequency (cm-1)with HF/ 6-31G			Calculated frequency (cm-1)with HF/ 6-31G (d,p)			Calculated frequency (cm-1)with HF/ 6-31+ + g(d, p)			Vibrational
	IR(cm^{-1})	Un-scaled (cm^{-1})	scaled (cm^{-1})	IR Intensity	Un-scaled (cm^{-1})	scaled (cm^{-1})	IR Intensity	Un-scaled (cm^{-1})	Scaled (cm^{-1})	IR Intensity	Un-scaled (cm^{-1})	scaled (cm^{-1})	IR Intensity	Un-scaled (cm^{-1})	scaled (cm^{-1})	IR Intensity	Un-scaled (cm^{-1})	scaled (cm^{-1})	IR Intensity	
1		55.77	54	1.53	55.08	53	2.23	52.22	50	2.28	55.01	50	3.57	53.53	48	4.12	15.30	14	3.95	ρ(C16C11C12)
2		70.65	68	4.61	69.88	67	2.99	67.44	65	4.13	73.14	66	4.75	73.71	67	2.62	70.86	64	3.51	γ(all structure)
3		129.72	125	5.04	123.73	119	4.38	121.34	117	4.26	138.7	125	6.07	132.52	120	5.23	130.0	117	4.70	γ(all structure)
4		131.35	127	0.14	129.79	125	0.03	138.53	134	0.19	148.2	134	0.18	153.03	138	0.03	155.2	140	0.06	ρ(C20H3)
5		178.76	173	0.52	176.17	170	0.39	174.47	168	0.50	191.4	173	0.48	188.40	170	0.36	186.9	169	0.45	β(C11C16C12)
6		195.32	189	0.31	186.26	180	0.36	185.68	179	0.37	207.5	187	0.44	198.72	179	0.48	199.0	180	0.42	ρ(C20H3), γ(O=C4C5ring)
7		237.17	229	0.12	236.52	228	0.09	232.83	225	0.11	250.8	227	0.20	251.40	227.	0.15	248.8	225	0.20	ρ(C12H3; C16H3)
8		257.91	249	0.18	252.76	244	0.08	248.34	240	0.09	281.3	254	0.42	271.93	246	0.16	267.6	242	0.13	ρ(C12H3), γ(O=C1C2ring)
9		266.93	258	0.04	268.72	259	0.02	265.13	256	0.04	291.58	263	0.01	298.07	269	0.01	295.50	267	0.02	ρ(C12H3; C16H3)
10		294.89	285	0.20	288.22	278	0.10	286.75	277	0.14	315.25	285	0.39	307.52	278	0.19	305.86	276	0.19	β(C6ring-C20H3)
11		303.15	293	3.38	296.32	286	2.67	295.52	285	2.31	324.776	293	3.66	316.86	286	2.82	315.92	285	2.66	β(C16C11C12), β(C6ring-C20H3)
12		400.45	386	4.49	384.69	371	0.37	384.18	371	0.91	436.52	394	9.16	415.45	375	0.40	413.25	373	0.73	γ(ring),ρ(C20H3), β(C12C11C16)
13		407.11	393	20.54	403.22	389	0.12	403.88	390	8.27	442.24	399	26.59	435.16	393	5.62	434.26	392	5.77	β(C=O)ring, β(C12C11C16)
14	409.7 m	415.08	401	0.42	405.31	391	22.45	404.92	391	13.33	450.18	407	1.18	439.74	397	25.56	438.68	396	24.19	β(C=O)ring, β(C12C11C16)
15	453.43 w	462.84	447	1.77	452.77	437	2.87	453.19	437	2.47	501.67	453	3.42	488.61	441	5.60	487.70	440	5.01	γ(CCC)ring, γ(C11H)
16		489.26	472	0.46	479.71	463	0.66	479.31	463	0.60	526.09	475	0.69	513.56	464	0.86	512.25	463	0.81	γ(CCC)ring,γ(CH)ring, ω(C12H3;C11H;C16H3)
17	515.8 w	535.93	517	1.20	522.82	505	1.68	522.56	504	1.55	577.84	522	2.27	563.62	509	3.10	562.60	508	2.80	γ(CCC)ring,γ(CH)ring, ω(C12H3;C11H;C16H3)
18		626.74	605	0.97	617.15	596	0.74	616.52	595	0.63	672.24	607	1.37	660.32	596	0.97	659.44	595	0.80	β(C5C6ring-C20H3), β(CCring-O), β(CH)ring
19	609.96 w	682.53	659	2.59	672.65	649	2.08	671.80	648	1.75	734.81	664	4.23	723.40	653	2.72	722.02	652	2.29	β(C=C-C)ring, ω(C12H3; C20H3)
20		703.43	679	2.67	693.24	669	2.66	691.33	667	2.50	750.85	678	3.79	740.15	668	3.60	738.25	667	3.36	Breath(ring)
21	705.77 m	722.76	697	5.43	712.80	688	5.67	711.14	686	4.84	781.82	706	11.56	772.11	697	10.53	768.92	694	8.75	γ(ring), ρ(C12H3;C16H3;C20H3)
22		796.61	769	0.36	792.42	765	0.28	788.96	761	0.21	865.26	781	0.82	862.81	779	0.52	854.20	771	0.56	γ(ring), γ(CH)ring
23		825.49	797	8.33	814.33	786	5.91	814.13	786	5.47	885.45	780	6.84	874.00	789	3.68	872.61	788	3.36	β(CH)ring, ϑ(C-C)ring ω(C12H3;C16H3;C20H3)
24	808.19 w	887.26	856	5.07	879.97	849	4.03	876.87	846	3.69	947.32	855	2.84	941.81	850	2.50	940.15	849	2.15	$\gamma(CH)ring, \rho$(C12H3;C16H3)
25		916.77	885	1.63	893.30	862	1.04	889.53	858	1.52	1010.92	913	3.90	977.23	882	1.67	970.47	876	2.64	γ(CH)ring
26		954.44	921	33.46	936.34	904	13.25	935.23	902	11.32	1041.81	941	2.90	1011.55	913	0.91	1010.03	912	0.82	γ(CH)ring, ω(C16H3)
27	870.73 w	965.17	931	8.56	940.28	907	22.17	939.46	907	29.17	1062.20	959	61.39	1036.32	936	58.13	1033.74	933	61.17	γ(CH)ring, ρ(C12H3; C16H3)
28		995.23	960	0.02	975.14	941	0.15	971.09	937	0.10	1064.53	961	4.31	1044.49	943	0.89	1042.12	941	0.70	$\boldsymbol{\rho}$(C12H3; C16H3)
29	932.98 m	1050.61	1014	5.43	1022.07	986	14.45	1021.23	985	17.13	1125.07	1016	3.82	1105.44	998	1.04	1104.18	997	0.78	$\boldsymbol{\omega}$(C20H3)

30	1024.28 m	1055.63	1019	42.03	1038.46	1002	30.55	1035.65	999	28.57	1142.88	1032	33.13	1117.64	1009	31.54	1115.83	1008	31.75	ϑ(**C3ring – C11**), ω(C12H3;C16H3;C20H3)
31		1097.02	1059	5.97	1062.02	1025	2.96	1059.52	1022	2.40	1201.34	1085	5.37	1162.28	1049	1.50	1159.72	1047	1.11	ρ(C20H3)
32		1132.43	1093	9.40	1115.10	1076	6.08	1110.46	1072	7.51	1221.39	1103	9.22	1203.23	1087	5.93	1200.78	1084	6.26	ω(C12H3), γ(C11H)
33		1153.93	1114	4.55	1131.45	1092	10.68	1126.71	1087	6.45	1248.55	1127	16.66	1223.07	1104	18.56	1220.65	1102	15.30	ω(C12H3;C16H3),β(C11H)
34	1104..31 w	1173.96	1133	31.85	1152.90	1113	32.13	1150.47	1110	36.33	1265.43	1143	22.80	1244.25	1124	25.07	1242.42	1122	26.61	β(CH) ring,ω(C12H3;C20H3)
35	1132.42 m	1228.64	1186	1.81	1207.06	1165	2.71	1202.13	1160	4.60	1330.19	1201	1.64	1308.14	1181	2.44	1305.09	1178	3.36	β(C11H), ω(C16H3; C12H3)
36	1179.75 w	1270.72	1226	22.62	1238.48	1195	3.53	1240.59	1197	4.07	1374.35	1241	123.42	1346.54	1216	0.57	1348.22	1217	0.64	β(CH)ring
37	1247.16 m	1276.93	1232	90.15	1265.70	1221	112.89	1262.43	1218	106.36	1379.13	1245	0.22	1369.76	1237	126.03	1366.05	1234	120.21	β(CH)ring, ϑ(C-C)ring
38		1352.14	1305	7.50	1329.27	1283	16.85	1323.66	1277	7.53	1469.08	1327	9.62	1449.65	1309	18.81	1446.51	1306	15.03	β(C11H), β(CH)ring
39		1353.15	1306	3.99	1332.78	1286	1.70	1327.13	1281	8.61	1472.55	1330	0.83	1457.42	1316	3.52	1452.84	1312	4.02	β(C11H)
40	1303.9 w	1399.63	1351	18.91	1376.64	1328	29.29	1372.77	1325	28.07	1519.14	1372	19.75	1501.04	1355	33.07	1498.03	1353	31.66	ϑ(C-C)ring, β(CH)ring, ω(C20H2)
41		1422.64	1373	4.66	1399.18	1350	1.17	1394.42	1346	1.39	1551.12	1401	2.85	1529.84	1381	1.42	1525.56	1378	1.89	δ_s(**C16H3; C12H3**), ϑ(C-C)ring, β(C11H)
42	1359.99 m	1444.55	1394	11.09	1414.43	1365	9.02	1409.26	1360	10.90	1568.77	1417	10.65	1545.73	1396	5.07	1541.82	1392	5.34	δ_s(C16H3;C12H3)
43		1462.93	1412	5.25	1426.77	1377	5.36	1421.41	1372	8.66	1587.83	1434	6.82	1558.18	1407	3.97	1553.63	1403	5.44	δ_s(C16H3;C12H3)
44		1464.14	1413	15.78	1430.24	1380	3.29	1423.35	1373	4.69	1589.78	1436	8.06	1560.83	1409	3.67	1556.51	1406	3.97	δ_s(C20H3)
45		1515.02	1462	10.20	1481.25	1429	7.17	1472.23	1421	8.97	1631.53	1473	9.84	1600.15	1445	6.40	1593.96	1439	7.90	δ_{as}(C20H3)
46	1437.06 w	1523.52	1470	8.16	1490.41	1438	9.42	1482.96	1431	10.49	1639.39	1480	9.67	1608.92	1453	9.21	1605.27	1450	9.92	δ_{as}(C20H3)
47		1534.05	1480	3.91	1503.20	1451	2.13	1493.22	1441	1.69	1647.82	1488	1.72	1618.28	1461	1.10	1611.84	1455	0.98	δ_{as}(C16H3;C12H3)
48		1537.13	1483	5.75	1505.91	1453	4.61	1496.81	1444	5.05	1651.35	1491	6.42	1922.26	1736	4.12	1616.32	1460	4.32	δ_{as}(C16H3;C12H3)
49		1551.84	1497	9.35	1520.45	1467	7.05	1511.43	1459	10.48	1666.23	1505	12.12	1636.35	1478	7.89	1630.57	1472	10.67	δ_{as}(C16H3;C12H3)
50	1461.3 w	1555.05	1501	13.62	1526.83	1473	7.34	1516.18	1463	10.93	1669.37	1507	10.73	1643.05	1484	5.63	1636.22	1478	6.87	δ_{as}(C16H3;C12H3)
51	1615.11 m	1633.83	1571	1.74	1673.18	1615	64.58	1662.52	1604	76.18	1835.44	1657	2.81	1851.63	1672	36.66	1838.57	1660	41.93	ϑ(C=C) ring
52		1657.04	1599	266.75	1707.52	1648	2.84	1693.27	1634	4.40	1855.23	1675	28.04	1878.72	1697	3.73	1865.03	1684	4.30	ϑ(Cring = O), ϑ(C=C) ring
53	1654.99 s	1675.36	1617	80.40	1739.90	1679	238.52	1719.58	1659	445.30	1882.82	1700	555.63	1980.18	1788	638.24	1959.37	1769	764.7	ϑ(Cring = O)
54		1723.85	1663	0.68	1745.11	1684	111.43	1726.59	1666	13.32	1934.68	1747	1.46	2001.16	1807	13.83	1982.53	1790	4.46	β(CCC)ring, ϑ(C=O)ring
55	2877.56 w	3042.57	2936	19.50	3042.26	2936	17.49	3036.23	2930	22.41	3189.13	2880	26.64	3182.75	2874	26.46	3179.12	2871	29.15	ϑ_s(C12-H3)
56	2928.12 w	3047.03	2940	32.42	3046.31	2940	23.13	3039.74	2933	28.34	3194.14	2884	30.72	3188.32	2879	30.59	3184.86	2876	32.75	ϑ(C11-H),ϑ_s(C16-H3),ϑ_s(C12-H2)
57		3054.48	2948	10.52	3054.02	2947	8.38	3049.07	2942	9.72	3206.67	2896	14.77	3201.14	2891	17.77	3199.53	2889	19.03	ϑ_s(C16-H3)
58		3055.14	2948	7.92	3056.24	2949	7.28	3054.12	2947	4.00	3222.93	2910	1.34	3223.43	2911	1.70	3219.28	2907	1.75	ϑ(C11-H)
59		3113.92	3005	11.09	3110.21	3001	8.55	3103.05	2994	5.96	3256.16	2940	2.42	3246.79	2932	3.30	3241.23	2927	4.23	ϑ_{as}(C12-H3), ϑ_{as}(C16-H2)
60		3114.54	3006	8.90	3112.39	3003	6.57	3106.51	2998	5.33	3266.33	2949	41.57	3258.25	2942	54.20	3252.94	2937	38.66	ϑ_{as}(C20-H2)
61	2969.52 m	3122.66	3013	38.17	3117.24	3008	41.29	3109.43	3001	44.90	3268.12	2951	65.44	3259.63	2943	63.28	3254.32	2939	79.44	ϑ_{as}(C12-H3),ϑ_{as}(C16-H2), ϑ(C11-H)
62		3127.05	3018	41.21	3112.59	3004	31.50	3114.67	3006	32.96	3273.19	2956	10.79	3267.07	2950	13.80	3264.51	2948	11.77	ϑ_{as}(C16-H3)
63		3148.53	3038	16.69	3144.03	3034	15.06	3132.72	3023	16.20	3289.41	2970	20.89	3281.61	2963	24.21	3274.25	2957	25.09	ϑ_{as}(C12-H3)
64		3151.46	3041	12.83	3146.74	3037	11.17	3139.93	3030	11.97	3294.13	2975	14.07	3286.32	2968	16.17	3282.73	2964	16.23	ϑ_{as}(C20-H3)
65	3050 w	3215.83	3103	6.86	3193.91	3082	6.57	3191.81	3080	6.00	3390.34	3061	3.87	3368.54	3042	4.52	3366.85	3040	4.21	ϑ(CH)ring
66		3229.97	3117	2.95	3207.18	3095	2.89	3206.22	3094	2.36	3409.27	3079	2.06	3387.62	3059	2.17	3387.13	3059	1.87	ϑ(CH)ring

ϑ: stretching, ϑ_s: symmetric stretching, ϑ_{as}: asymmetric stretching, δ_s: symmetric bend, δ_{as}: anti-symmetric bend, γ: out of plane bending, β: in plane bending, ω: wagging, ρ: rocking, w: weak, m: medium, s: strong.
*Experimental from reference [25]

Table 2. Mean percentage error (MPE), mean absolute error (MAE) and root mean square error (RMSE) from experimental fundamentals with different basis sets

Method	Basis Set	MPE %		MAE		RMSE	
		Un-scaled	Scaled	Un-scaled	Scaled	Un-scaled	Scaled
HF	6 – 31G	14.04	3.32	181.61	37.09	198.22	47
	6 – 31G(d,p)	12.81	3.05	171.08	34.25	191.42	44.61
	6 – 31+ + G(d,p)	12.53	2.95	167.3	29.59	187	41.22
DFT/B3LYP	6 – 31G	5.71	3	75.46	35.25	89.66	40.86
	6 – 31G(d,p)	4.56	2.29	64.8	23.73	78.98	28.25
	6 – 31+ + G(d,p)	4.28	2.18	60.45	21.64	74.65	26.28

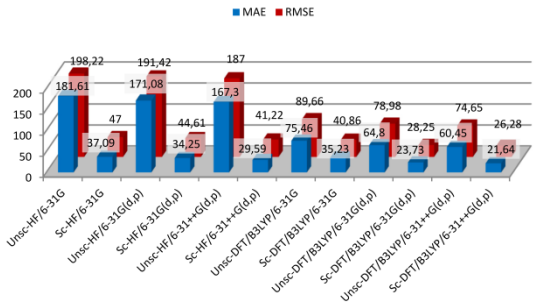

Figure 2. Histogram of RMSE and MAE of the title compound for the un-scaled and scaled HF and DFT/B3LYP methods, at various basis sets

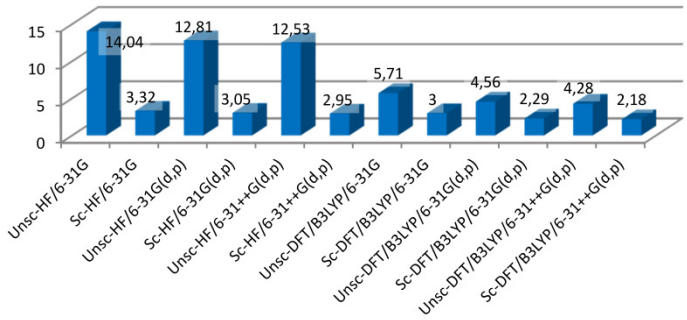

Figure 3. Histogram of MPE of the title compound for the un-scaled and scaled HF and DFT/B3LYP method, at various basis sets

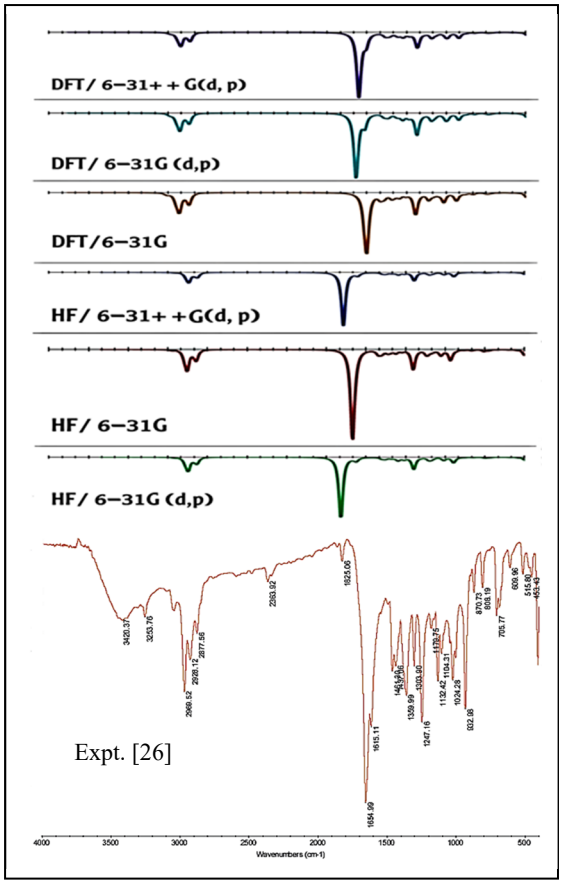

Figure 4. Experimental (from ref [25]) and calculated (scaled) IR spectra of the title compound

UV-Visible absorption spectra

The UV-Visible absorption spectra analysis of Thymoquinone compound have been studied by theoretical calculations under the same optimization conditions that were previously mentioned in this article. The calculated results

including the maximum absorption wavelengths (λ_{max}), oscillator strengths (f), molecular orbitals undergoing transitions, vertical excitation energy, the major contributions, and the experimental wavelength are shown in the Table 3 and the UV-Visible spectra of the title compound as obtained from TD-DFT method at several basis sets with experimental spectrum are shown in Figure 5. According the results obtained in the UV-Visible theoretical spectra, the theoretical model that appear the best agreement, is HF method with 6-31G basis set that estimates the λ_{max} about 249 nm in relation to the 254 nm experimental maximum absorption wave length reported by M.S. Iqbal, et al. [14]. It is seen from Table 4, calculations performed at HF/6-31G method in best agreement with the experimental result compared to the DFT/B3LYP method and other basis sets. The electronic transition is represented as a result of the contribution of the highest occupied molecular orbital to the lowest unoccupied molecular orbital (HOMO→LUMO) with the absorption wavelength, which implies the transfer of electron density as ($\pi \rightarrow \pi^*$) transition with 91% donating.This electronic absorption is mainly described at the maximum absorption wavelength249 nm by electronic excitation from HOMO to LUMO and corresponds to the transition from the ground state to the first excited state. The maximum absorption peak (λ_{max}) optimized by HF/6-31G level reduces the error to 5 nmıo While for the rest of the basis sets, especially for the DFT method, the difference is large. These outcomes demonstrate it is not necessary that the same computational method for all calculations, for example, IR and UV-Vis spectra, agree with the experimental results.

Table 3. The experimental and calculated maximum absorption wavelength (λ_{max}) excitation energies and oscillator strengths of the title compound.

Basis sets	**The calculated with TD-DFT/-HF in gas phase**					**The calculated with TD-DFT/B3LYP in gas phase**				
	wavelength λ_{max}(nm)	Energy (ev)	Osc. Strenght	Major Contribution	Transition	wavelength λ_{max}(nm)	Energy (ev)	Osc. Strenght	Major Contribution	Transition
6-31G	249.39	4.9608	0.0008	HOMO->LUMO 90.9%	$\pi \rightarrow \pi^*$	372.74	3.3263	0.0004	HOMO-2->LUMO 97.3%	$\pi \rightarrow \pi^*$
6-31G(d,p)	240.82	5.1483	0.0007	HOMO->LUMO 93.5%	$\pi \rightarrow \pi^*$	356.6	3.4768	0.0004	HOMO -2-> LUMO 97.8%	$\pi \rightarrow \pi^*$
6-31G++(d,p)	245.83	5.0434	0.0007	HOMO->LUMO 92.6%	$\pi \rightarrow \pi^*$	357.53	3.4678	0.0005	HOMO -2-> LUMO 96.9%	$\pi \rightarrow \pi^*$
Experimental[**]	254 nm									

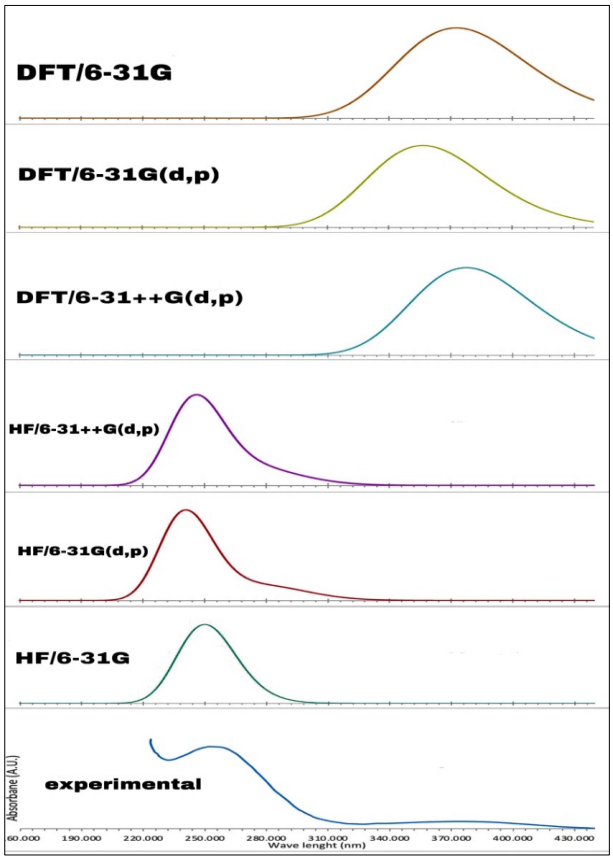

Figure 5. Experimental (from reference [14]) and calculated UV-Vis spectra of the title compound

CONCLUSION

In this study, the FT-IR and UV-Vis spectra of the compound thymoquinone (TQ) have been calculated by two chemical models DFT/B3LYP and HF using 6-31G, 6-31G(d,p) and 6-31++G(d,p) basis sets and compared with

experimental results. Also, the present study aims to explore the performances two chemical models regarding statistical analysis of IR vibrational frequencies for the title compound, using root mean square error (RMSE), mean absolute error (MAE) and mean percentage error (MPE) calculations to give numerical estimates of these performances. The performed statistical analysis between computed and experimental vibrational frequencies showed the best performance of DFT/B3LYP method, especially with large basis sets. The DFT/B3LYP method with 6-31++G(d,p) basis set for predicting vibrational frequencies was the most successful procedure. Furthermore, it was found the theoretical scaled vibrational frequencies by DFT/B3LYP method with 6-31++G(d,p) basis set showed good agreement with the experimental data. Although DFT/B3LYP performs well for vibrational frequencies, it is less efficient for UV-Visible spectrum, where the best results were obtained for the maximum absorption wavelength through the HF method with the basis set 6-31G. These outcomes demonstrate it is not necessary that the same computational method for all calculations, for example, IR, UV-Visand NMR spectra, agree with the experimental results.

ORCID IDs

Salah M.A. Ridha, https://orcid.org/0000-0003-0569-3849; **Zahraa Talib Ghaleb**, https://orcid.org/0000-0003-0569-3849
Abdulhadi Mirdan Ghaleb, https://orcid.org/0000-0002-2202-8827

REFERENCES

[1] B.H. Ali, and G. Blunden, "Pharmacological and toxicological properties of Nigella sativa", Phytother. Res. **17**, 299-305 (2003). https://doi.org/10.1002/ptr.1309
[2] Z. Erisgin, M. Atasever, K. Cetinkaya, S.A. Dizakar, S. Omeroglu, and H. Sahin, "Protective effects of, Nigella sativa oil against carboplatin-induced liver damage in rats", Biomedicine & Pharmacotherapy, **110**, 742-747 (2019). https://doi.org/10.1016/j.biopha.2018.12.037
[3] P.K. Perera, D.T. Karunaratne, and N. Kalka, *Antiinflammatory Actions and Potential Usage for Arthritic Conditions, Bioactive Food as Dietary Interventions for Arthritis and Related Inflammatory Diseases*, (2nd edition), (Academic Press, 2019), pp. 323-341. https://doi.org/10.1016/B978-0-12-813820-5.00019-2
[4] M. El-Dakhakhny, "Studies on the Egyptian Nigella sativa L. IV. Some pharmacological properties of the seeds' active principle in comparison to its dihydro compound and its polymer", Arzneimittel-forsch, **15**(10), 1227–1229 (1965).
[5] M.E. Abd El-Hack, M. Alagawany, M.R. Farag, R. Tiwari, K. Karthik, and K. Dhama, "Nutritional, Healthical and Therapeutic Efficacy of Black Cumin (Nigella sativa) in Animals, Poultry and Humans", International Journal of Pharmacology, **12**, 232-248 (2016). https://doi.org/10.3923/ijp.2016.232.248
[6] H. Mollazadeh, A.R. Afshari, and H. Hosseinzadeh, "Review on the Potential Therapeutic Roles of Nigella sativa in the Treatment of Patients with Cancer: Involvement of Apoptosis: Black cumin and cancer", J. Pharmacopuncture, **20**(3), 158-172 (2017). https://doi.org/10.3831%2FKPI.2017.20.019
[7] M.A. Randhawa, M. Al-Ghamdi, M. Al-Ghamdi, "Anticancer Activity of Nigella sativa (Black Seed) - A Review", The American Journal of Chinese Medicine, **39**(6), 1075 (2011). https://doi.org/10.1142/S0192415X1100941X
[8] D.R. Worthen, O.A. Ghosheh, P.A. Crooks, "The in vitro anti-tumor activity of some crude and purified components of blackseed, Nigella sativa L", Anticancer Res. **18**, 1527-1532 (1998).
[9] M. Burits, F. Bucar, "Antioxidant activity of Nigella sativa essential oil", Phytotherapy Research, **14**, 323-328 (2000). https://doi.org/10.1002/1099-1573(200008)14:5%3C323::AID-PTR621%3E3.0.CO;2-Q
[10] P.J. Houghton, R. Zarka, B. de la Heras, J.R.S. Hoult, "Fixed oil of Nigella sativa and derived thymoquinone inhibit eicosanoid generation in leukocytes and membrane lipid peroxidation", Planta Medica, **61**, 33-36 (1995). https://doi.org/10.1055/s-2006-957994
[11] N.M. Morsi, "Antimicrobial effect of crude extracts of Nigella sativa on multiple antibiotics-resistant bacteria", Acta Microbiologica Polonica, **49**, 63-74 (2000).
[12] M.L. Salem, and M.S. Hossain, "In vivo acute depletion of CD8(+) T cells before murine cytomegalovirus infection upregulated innate antiviral activity of natural killer cells", International Journal of Immunopharmacology, **22**, 707-718 (2000). https://doi.org/10.1016/S0192-0561(00)00033-3
[13] A.H. Gilani, N. Aziz, I.M. Khurram, K.S. Chaudhary, A. Iqbal, "Bron-chodilator."Spasmolytic and Calcium Antagonist Activities of Nigella sativa seeds (Kalonji): a traditional herbal product with Multiple Me-dicinal Uses", J. Pak. Med. Assoc. **51**, 115-119 (2001). https://ecommons.aku.edu/pakistan_fhs_mc_bbs/422
[14] M.S. Iqbal, A. Jafri, Md. Arshadb, and M.I. Ansari, "Stress response due to sodium azide treatment inside Nigella sativa L. plant and its effect on antioxidative property", Biocatalysis and Agricultural Biotechnology, **19**, 101171 (2019). https://doi.org/10.1016/j.bcab.2019.101171
[15] C. Moller, and M.S. Plesset,"Note on an Approximation Treatment for Many-Electron Systems", Phys. Rev. **46**, 618–622 (1934). https://doi.org/10.1103/PhysRev.46.618
[16] A.D. Becke, "Density-Functional Exchange-Energy Approximation with Correct Asymptotic-Behavior", Phys. Rev. A, **38**(6), 3098–3100 (1988). https://doi.org/10.1103/PhysRevA.38.3098
[17] C.T. Lee, W.T. Yang, and R.G. Parr, "Development of the Colle-Salvetti Correlation-Energy Formula into a Functional of the Electron-Density", Phys. Rev. B, **37**(2), 785–789 (1988). https://doi.org/10.1103/PhysRevB.37.785
[18] M.J. Frisch, G.W. Trucks, H.B. Schlegel, G.E. Scuseria, M.A. Robb, J.R. Cheeseman, J.A. Montgomery, et al, *Gaussian 03, Revision C.02*, (Gaussian, Inc, Wallingford CT, 2004).
[19] R. Denning, T. Keith, J. Millam, K. Eppinnett, W. Hovell, and R.G. Gilliland, *Version 3.09*, (Semichem. Inc., Shawnee Mission, KS, 2003).
[20] M.A. Palafox, "DFT computations on vibrational spectra: Scaling procedures to improve the wavenumbers", Physical Sciences Reviews, **3**(6), 20170184 (2018). https://doi.org/10.1515/psr-2017-0184
[21] *Integrated Spectral Data Base System for Organic Compounds*, (Ibaraki, Japan, National Institute of Advanced In-dustrial Science and Technology, 2003).

[22] Y. Yamakita, and M. Tasumi, "Vibrational analyses of p-benzoquinodimethane and p-benzoquinone based on ab initio Hartree-Fock and second-order Moller-Plessetcalculations", J. Phys. Chem. **99**, 8524-8534(1995). https://doi.org/10.1021/j100021a013
[23] R. Gupta, "Study of spectral and NLO properties of 2-methyl-5-(Propan-2-yl) phenol by DFT", IJSRED, **4**(3), 689-705 (2021). http://www.ijsred.com/volume4/issue3/IJSRED-V4I3P94.pdf
[24] K.M. Marzec, I. Reva, R. Fausto, and L.M. Proniewicz, "Comparative Matrix Isolation Infrared Specroscopy Study of 1,3- and 1,4- DieneMonoterpenes (α- Phellandrene and γ-Terpinene)", J. Phys. Chem. A, **115**, 4342-4353 (2011). https://doi.org/10.1021/jp2013122
[25] R. Abu-Dahab, F. Odeh, S.I. Ismail, H. Azzam, and A. Al Bawab, "Preparation, characterization and antiproliferative activity of thymoquinone-β-cyclodextrin self-assembling nanoparticles", Pharmazie, **68**, 939–944 (2013). https://doi.org/10.1691/ph.2013.3033

ОБЧИСЛЮВАЛЬНЕ ДОСЛІДЖЕННЯ IR ТА UV-VIS СПЕКТРІВ 2-ІЗОПРОПІЛ-5-МЕТИЛ-1,4-БЕНЗОХІНОНУ ЗА ДОПОМОГОЮ МЕТОДІВ DFT ТА HF

Салах М.А. Рідха[a], Захра Таліб Галеб[b], Абдулхаді Мірдан Галеб[a]

[a]Департамент фізики наукового коледжу, Кіркукського університету, Кіркук, Ірак
[b]Департамент хімії наукового коледжу Кіркукського університету, Кіркук, Ірак

Проведено теоретичне дослідження сполуки тимохінону за допомогою двох теоретичних методів, DFT/B3LYP і HF з базовими наборами 6-31G, 6-31G(d,p) і 6-31++G(d,p) з використанням програми Гауссіан 09. Деякі теоретичні властивості, такі як вібраційні та електронні властивості, особливо UV-vis та IR-спектри, були проаналізовані, а потім порівняні з доступними експериментальними даними. Розраховані частоти гармонійних коливань були масштабовані зі стандартними коефіцієнтами масштабування 0,9 і 0,965 для HF і DFT/B3LYP відповідно, а потім порівняні з наявним експериментальним спектром FT-IR. Крім того, було досліджено статистичний аналіз для оцінки ефективності методів HF і DFT, включаючи середньоквадратичну помилку (RMSE), середню абсолютну помилку (MAE) і середню помилку у відсотках (MPE). Відповідно до призначених вібраційних режимів сполуки, можна зробити висновок, що метод DFT/B3LYP з базовим набором 6-31++G(d,p) мав найкращу узгодженість з експериментальними даними. Спектри поглинання в УФ-видимому діапазоні, енергії збудження, максимальну довжину хвилі поглинання, електронні переходи та сили осциляторів зазначеної в заголовку сполуки розраховували методом залежної від часу теорії функціоналу щільності (TD-DFT) з використанням того самого базового набору та порівнювали з наявними експериментальними даними. Результати показали, що найкращим результатом був ВЧ-метод із базовим набором 6-31G.

Ключові слова: *тимохінон; DFT; HF; UV-Vis; FT-IR; TD-DFT*